

## **Potential Remediation Approach for Uranium-contaminated Groundwaters Through Potassium Uranyl Vanadate Precipitation**

Tetsu K. Tokunaga, Yongman Kim, and Jiamin Wan

Earth Sciences Division, Lawrence Berkeley National Laboratory

Berkeley, California

Methods for remediating groundwaters contaminated with uranium (U) through precipitation under oxidizing conditions are needed because bioreduction-based approaches require indefinite supply of electron donor. Although strategies based on precipitation of some phosphate minerals within the (meta)autunite group have been considered for this purpose, thermodynamic calculations for K- and Ca-uranyl phosphates, meta-ankoleite and autunite, predict that U concentrations will exceed the Maximum Contaminant Level (MCL = 0.13  $\mu\text{M}$  for U) at any pH and  $\text{pCO}_2$ , unless phosphate is maintained at much higher concentrations than the sub- $\mu\text{M}$  levels typically found in groundwaters. We hypothesized that potassium uranyl vanadate will control U(VI) concentrations below regulatory levels in slightly acidic to neutral solutions based on thermodynamic data available for carnotite,  $\text{K}_2(\text{UO}_2)_2\text{V}_2\text{O}_8$ . The calculations indicate that maintaining U concentrations below the MCL through precipitation of carnotite will be sustainable in some oxidizing waters having pH in the range of 5.5 to 7, even when dissolution of this solid phase becomes the sole supply of sub- $\mu\text{M}$  levels of V. Batch experiments were conducted in solutions at pH 6.0 and 7.8, chosen because of their very different predicted extents of U(VI) removal. Conditions were identified where U

concentrations dropped below its MCL within 1 to 5 days of contact with oxidizing solutions containing 0.2 to 10 mM K, and 0.1 to 20  $\mu\text{M}$  V(V). This method may also have application in extracting (mining) U and V from groundwaters where they both occur at elevated concentrations.

## **Introduction**

Uranium has become an important contaminant at numerous sites where it has been mined and processed for nuclear energy and weapons development. High costs associated with excavating and safely disposing U-contaminated soils and sediments have prompted research into in situ remediation strategies. Because of the typically much lower solubility of uraninite ( $\text{UO}_2$ ) and even amorphous  $\text{UO}_2$  relative to U(VI) minerals (1), reduction-based remediation methods are being developed by a number of research groups, with most efforts exploring microbially mediated reduction of soluble uranyl species (2, 3). Although bioreduction can lower aqueous U concentrations below regulatory limits (the U.S. Environmental Protection Agency's Maximum Contaminant Level, MCL, for U is 0.13  $\mu\text{M}$ ), recent studies have identified several potential problems with this approach. Elevated concentrations of bicarbonate and organic ligands from microbial utilization of organic carbon promote higher aqueous U(VI) concentrations because of the high stability of U(VI) carbonate (4) and organic complexes (5), even under reducing conditions. Therefore, the rate of organic carbon supplied in a bioreduction based approach to U stabilization must be high enough to maintain reducing conditions yet low enough to minimize formation of aqueous U(VI) carbonates (4, 6, 7). Such fine-tuning of organic carbon supply rate is unlikely to be achievable in

the field because of hydrogeological and biogeochemical heterogeneity of the subsurface. Moreover, in light of evidence for fairly rapid U dissolution when oxidizing solutions return (8-10), bioreduction-based U stabilization is unsustainable because reducing conditions must be maintained in perpetuity. Given the impracticality of permanently establishing reducing conditions in regionally oxidizing environments, consideration of possible approaches to precipitating low solubility U(VI) solids warrant evaluation.

The mineralogy of oxidizing U ore deposits provides guidance in selecting potentially useful solubility-controlling minerals. For example, phosphate-containing autunite and meta-autunites comprise a major group of U(VI) minerals with solubilities below that of schoepite under some conditions. Recent studies have described various geochemical and microbially-mediated processes leading to precipitation of low solubility U(VI) phosphates of Na, K, Ca, Cu, and Ba (11-16). While phosphate-based in-situ U remediation strategies are being tested, the complex chemistry and mineralogy of U suggests that other target solid phases are also worth examination for even better control of aqueous U concentrations.

Based on the importance of carnotite,  $K_2(UO_2)_2V_2O_8$ , and tyuyamunite,  $Ca(UO_2)_2V_2O_8$ , in some oxidized U ore deposits (1, 17-19), low solubility uranyl vanadates might also be effective for controlling aqueous U concentrations in contaminated sediments. Vanadate in these minerals occurs in paired, edge-sharing square pyramids within uranyl vanadate sheet structures. In sediments and groundwaters, vanadium occurs in the III, IV, and V (vanadate) oxidation states, with V(V) species being dominant at and above moderately oxidizing pe (17, 20). Typical

soils and sediments contain V at concentrations ranging from about 3 to 300 mg kg<sup>-1</sup> (21). Data on groundwater V concentrations are limited, but a summary from the U.S. National Water-Quality Assessment Program (22) reported a median and maximum concentrations of 1.4 µg L<sup>-1</sup> (0.03 µM) and 190 µg L<sup>-1</sup> (3.7 µM), respectively (N = 835). No regulatory limit (MCL) on its concentration in drinking water have been set by the U.S.E.P.A., although V is currently on its Contaminant Candidate List (23). Sorption onto Fe oxides (24, 25) is important in moderating aqueous V(V) concentrations, and therefore controls its subsurface transport. At low (µM) concentrations typical of groundwaters, vanadate occurs primarily as an oxyanion similar to phosphate, with H<sub>2</sub>VO<sub>4</sub><sup>-</sup> being the dominant species over the pH range of 3.8 to 8.0. Barton (26) provided brief descriptions of various procedures for carnotite synthesis, with attention primarily given to fusion methods conducted at elevated temperature. We found no accounts of K- or Ca- uranyl vanadate precipitation under conditions representative of near-surface groundwaters. Therefore, we initiated studies on U stabilization through precipitation of U(VI) vanadates in oxidizing solutions and soils. In the work presented here, we compare calculated U(VI) concentrations controlled by carnotite and tyuyamunite, to their (meta)autunite group (27) counterparts meta-ankoleite, (K<sub>2</sub>(UO<sub>2</sub>)<sub>2</sub>(PO<sub>4</sub>)<sub>2</sub>•6H<sub>2</sub>O) and autunite (Ca(UO<sub>2</sub>)<sub>2</sub>(PO<sub>4</sub>)<sub>2</sub>•10-12H<sub>2</sub>O), under conditions relevant to oxidizing groundwaters. We also present results from batch experiments on precipitation of U(VI) with K<sup>+</sup> and V(V) in aqueous solutions for comparison with equilibrium predictions.

## Materials and Methods

**Equilibrium calculations.** Uranium concentrations in equilibrium with meta-ankoleite, autunite, carnotite, and tyuyamunite were calculated using PHREEQC 2.12 (28). Solutions were modeled with a range of K, Ca, V, and P concentrations, in equilibrium with the atmosphere ( $p\text{CO}_2 = 3.5$ ) and with a moderately elevated  $p\text{CO}_2 = 2.5$  representative of slightly reducing pore waters. The majority of calculations were conducted with representative groundwater concentrations of  $\text{Ca}^{2+} = 1 \text{ mM}$ , and  $\text{K}^+ = 0.1 \text{ mM}$  (1). Thermodynamic data were taken from the Nuclear Energy Agency compilation (29) and other sources (1, 30-32). Standard molar Gibbs energies of formation for major species involved in calculations are listed in Table 1.

**Aqueous solution batch experiments.** From the equilibrium calculations shown later, carnotite and tyuyamunite control U concentrations to similar extents. However, tyuyamunite is the less common uranyl vanadate mineral, with only an estimated value available for its Gibbs free energy of formation (1). Thus, this initial set of experiments focused only on precipitation of carnotite. Based on the thermodynamic calculations, experiments were conducted at pH of 6.0 and 7.8. These two pH values were predicted to be near-optimal (lowest U concentration) and marginal (negligible U concentration change), respectively. Batch experiments were performed to determine extents of homogeneous U(VI) precipitation from solutions in response to additions of  $\text{K}^+$  and V(V), in order to form  $\text{K}_2(\text{UO}_2)_2\text{V}_2\text{O}_8$ . Uranyl nitrate (Spectrum Chemical) was used to prepare stock U(VI) solutions. Among commonly available vanadate compounds, potassium metavanadate,  $\text{KVO}_3$  (Aldrich), was selected because it required little pH adjustment for our tested range, and it includes  $\text{K}^+$ . Upon dissolution in water at dilute concentrations, dissociated  $\text{VO}_3^-$  converts to  $\text{H}_2\text{VO}_4^-$  (31). Samples

were prepared in duplicate 40 mL batches in screw cap Teflon vials, to contain  $\approx 1 \mu\text{M}$  U, with  $\text{K}^+$  concentrations of 0.1, 0.19, 1.0, and 10 mM, V(V) concentrations from 0 to 500  $\mu\text{M}$ , and  $\text{NaNO}_3$  added to set the ionic strength equal to 100 mM. Inclusion of nitrate also ensured that solutions remained oxidizing. The pH values of 6.0 and 7.8 were established using 1 mM 2-(N-morpholino)ethanesulfonic acid (MES) buffer (33, 34) and 1 mM  $\text{NaHCO}_3$ , respectively. Subsequent measurements indicated that solutions remained within  $\pm 0.1$  pH units throughout the experiments. Capped vials were continuously agitated on a reciprocating shaker ( $\approx 1 \text{ cycle s}^{-1}$ ) maintained at room temperature ( $20 \pm 1^\circ\text{C}$ ), and sampled at prescribed times from 1 day up to 50 days. At sampling times, vials were temporarily opened to withdraw 1 mL samples, which were then centrifuged (14000 relative centrifugal force for 60 minutes). Supernatant solutions were withdrawn after centrifugation for U analysis by kinetic phosphorescence analysis (KPA, Chemchek), and K and V analysis by ICP-OES. In all of these batch experiments, the KPA detection limit was 0.2 nM.

species	$\Delta G_f^\circ$ kJ/mol	source
$\text{UO}_2^{2+}$	-952.6	G
$\text{UO}_2\text{CO}_3^\circ$	-1537.2	G
$\text{UO}_2(\text{CO}_3)_2^{2-}$	-2103.2	G
$\text{UO}_2(\text{CO}_3)_3^{4-}$	-2660.9	G
$(\text{UO}_2)_2\text{CO}_3(\text{OH})_3^-$	-3139.5	G
$\text{CaUO}_2(\text{CO}_3)_3^{2-}$	-3231.8	DB
$\text{Ca}_2\text{UO}_2(\text{CO}_3)_3^\circ$	-3817.1	DB
$\text{UO}_2\text{OH}^+$	-1159.7	G
$\text{UO}_2(\text{OH})_2$	-1357.5	G
$\text{UO}_2(\text{OH})_3^-$	-1548.4	G
$\text{UO}_2(\text{OH})_4^{2-}$	-1716.2	G
$(\text{UO}_2)_2\text{OH}^{3+}$	-2126.8	G
$(\text{UO}_2)_2(\text{OH})_2^{2+}$	-2347.3	G
$\text{UO}_2\text{Cl}^+$	-1084.7	G
$\text{UO}_2\text{Cl}_2$	-1208.7	G
$\text{UO}_2\text{PO}_4^-$	-2040.8	R
$\text{UO}_2\text{HPO}_4$	-2089.9	G
$\text{UO}_2\text{H}_2\text{PO}_4^+$	-2108.3	G
$\text{UO}_2(\text{H}_2\text{PO}_4)_2$	-3254.9	G
$\text{UO}_2(\text{H}_2\text{PO}_4)(\text{H}_3\text{PO}_4)^+$	-3260.7	G
Meta-ankoleite, (K-autunite)	-4793.2	Lan
Autunite (Ca-autunite)	-4763.9	Lan
Carnotite	-4589.8	Lan
$\text{H}_2\text{O}$	-237.14	G
$\text{OH}^-$	-157.22	G
$\text{HCO}_3^-$	-586.85	G
$\text{CO}_3^{2-}$	-527.9	G
$\text{Cl}^-$	-131.217	G
$\text{NO}_3^-$	-110.79	G
$\text{H}_2\text{PO}_4^-$	-1137.15	G
$\text{HPO}_4^{2-}$	-1095.98	G
$\text{H}_2\text{VO}_4^-$	-1022.5	Lar
$\text{HVO}_4^{2-}$	-972.5	Lar
$\text{Na}^+$	-261.953	G
$\text{K}^+$	-282.51	G
$\text{Ca}^{2+}$	-552.81	G

**Table 1.** Thermodynamic constants for major species (298.15 K) used for calculating U concentrations. Sources: (G) Guillaumont et al. (29), (Lan) Langmuir (1), (Lar) Larson (31), (R.) Rai et al. (32), and (DB) from log K of Dong and Brooks (30), combined with  $\Delta G_f^\circ$  values from Guillaumont et al.

## Results and Discussion

**Equilibrium calculations.** Meta-ankoleite and autunite can lower U(VI) concentrations below the U-MCL when  $p\text{CO}_2$  is in equilibrium with the atmosphere and phosphate concentrations are sufficiently elevated. The calculations including a  $p\text{CO}_2$  of 3.5 and a total P of 100  $\mu\text{M}$  (very elevated relative to most groundwaters), indicate that U concentrations can be controlled below the MCL with autunite only over a narrow range of pH from 6.2 to 7.3 in the reference groundwater (0.1 mM  $\text{K}^+$  and 1 mM  $\text{Ca}^{2+}$ ), and that this control is lost when the  $\text{CO}_2$  partial pressure becomes elevated above equilibrium with the atmosphere (Figure 1). The increased concentrations of U through formation of various carbonate complexes is evident from comparing the  $p\text{CO}_2 = 3.5$  and 2.5 curves at neutral and high pH.

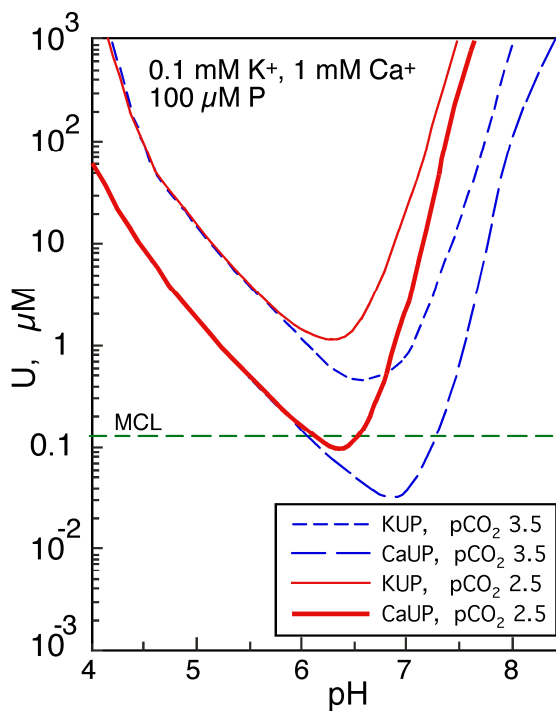


**Figure 1.** Uranium concentrations in equilibrium with  $p\text{CO}_2 = 3.5$  and 2.5, 0.1 mM  $\text{K}^+$  and 1.0 mM  $\text{Ca}^{2+}$ , ionic strength (I) = 100 mM for meta-ankoleite (KUP) and autunite (CaUP) with 100  $\mu\text{M}$  total phosphate



The U concentrations were calculated for conditions similar to those shown previously, but now with 1  $\mu\text{M}$  vanadate in equilibrium with carnotite (Figure 2a) and tyuyamunite (Figure 2b). Recall that the (meta)autunite equilibrium calculations were done with 100  $\mu\text{M}$  phosphate. Relative to their (meta)autunite counterparts, carnotite and tyuyamunite clearly control U concentrations below the MCL over a broader circum-neutral pH range more effectively when compared at equal concentrations of total P versus total V. Although we have used a newer thermodynamic database, many of these results are similar to those presented in Langmuir's comprehensive earlier paper (19). Enhanced U solubility through carbonate complex formation is again evident from comparing the  $\text{pCO}_2$  3.5 and 2.5 curves in Figure 2. Effects of varying levels of  $\text{Ca}^{2+}$  on dissolved U concentrations are shown in these diagrams for equilibrium with carnotite and tyuyamunite. In both carnotite (Figure 2a) and tyuyamunite (Figure 2b), increased  $\text{Ca}^{2+}$  concentrations stabilize U at higher concentrations in the higher pH range through formation of strong Ca-U-carbonate complexes  $\text{CaUO}_2(\text{CO}_3)_3^{2-}$  and  $\text{Ca}_2\text{UO}_2(\text{CO}_3)_3$  (30). Also shown in the acidic to intermediate pH range of Figure 2b is the effect of  $\text{Ca}^{2+}$  in driving U concentrations lower because it is a component of tyuyamunite. The combined effects of carbonates and  $\text{Ca}^{2+}$  on U(VI) complexation are predicted to maintain U concentrations above the MCL at  $\text{pH} > 7.5$ , even in the presence of 1  $\mu\text{M}$  V(V). Thus, in alkaline systems, pH neutralization is a prerequisite for controlling U(VI) concentrations through precipitation of either carnotite or tyuyamunite.

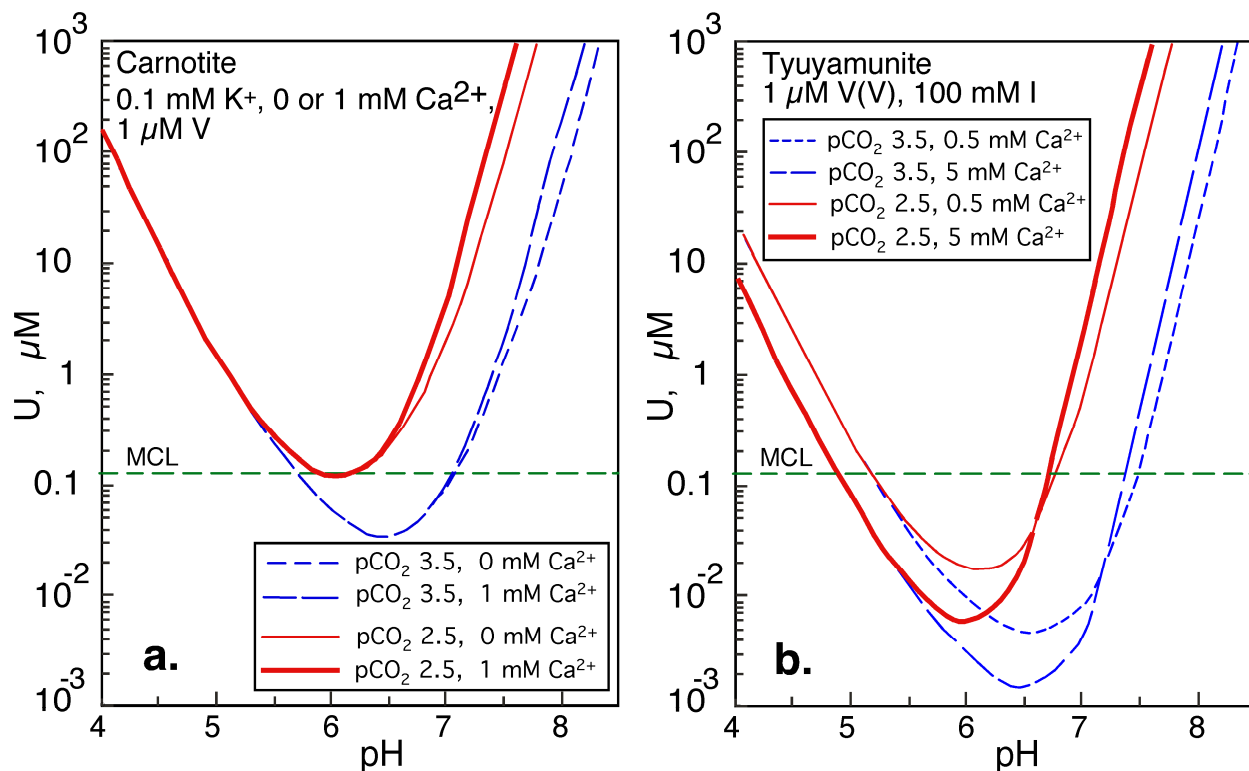


**Figure 2.** Uranium concentrations at  $\text{pCO}_2 = 3.5$  and  $2.5$ ,  $1 \text{ } \mu\text{M V(V)}$ , and  $\text{I} = 100 \text{ mM}$ , for equilibrium with (a.) carnotite ( $0.1 \text{ mM K}^+$ ;  $0$  and  $1 \text{ mM Ca}^{2+}$ ), and (b.) tyuyamunite ( $0.5$  and  $5.0 \text{ mM Ca}^{2+}$ ).

Important long-term conditions to consider involving (meta)autunite and uranyl vanadate solid phases are those where P and V concentrations are not fixed at single values, but instead are controlled by the dissolution of their uranyl minerals. Such conditions would apply in environments where meta-ankoleite, autunite, carnotite or tyuyamunite have precipitated naturally or as a result of remediation treatment, and subsequently begin to dissolve in groundwaters with low P, V, and U concentrations. In these cases, maximum component concentrations are determined by dissolution equilibria of the precipitated minerals. Calculations for such conditions are useful because they provide estimates of long term aqueous U(VI) concentrations associated

with contaminated sediments following precipitation of uranyl minerals and subsequent leaching by regional groundwaters. Cases for equilibrium U concentrations resulting from dissolution of meta-ankoleite and autunite under our reference conditions (0.1 mM  $K^+$ , 1 mM  $Ca^{2+}$ ,  $pCO_2$  4.5 and 2.5) are shown in Figure 3b. Because P concentrations are now limited by meta-ankoleite and autunite dissolution, U concentrations over the range of environmentally relevant pH are greatly elevated relative to the previously shown cases with fixed total phosphate = 100  $\mu M$ . Moreover these equilibrium concentrations all greatly exceed the U MCL. Therefore, kinetic limitations on dissolution would need to be important in order for these phosphate minerals to be useful in remediating U-contaminated sediments.

Predicted U concentrations in the reference groundwater from equilibrium dissolution of carnotite as the sole source of U and V are shown in Figure 3b. When carnotite dissolution provides the only source of U and V, comparisons with the fixed [V] cases (Figure 2a) reflect solubility product effects. Uranium concentrations are increased within the pH range of 5.1 to 6.7 ( $pCO_2$  2.5) or 7.4 ( $pCO_2$  3.5), where it was less than the fixed 1  $\mu M$  level of V concentration. Conversely, U concentrations are moderated at more extreme pH because of progressively higher  $[\Sigma V] = [\Sigma U]$  supplied by carnotite dissolution. These calculations with both U and V supplied only by carnotite dissolution predict that the U MCL will be approached, but slightly exceeded in this reference groundwater. Within the  $5 < pH < 7$  range, expected U concentrations exceed the MCL by less than 1  $\mu M$ .

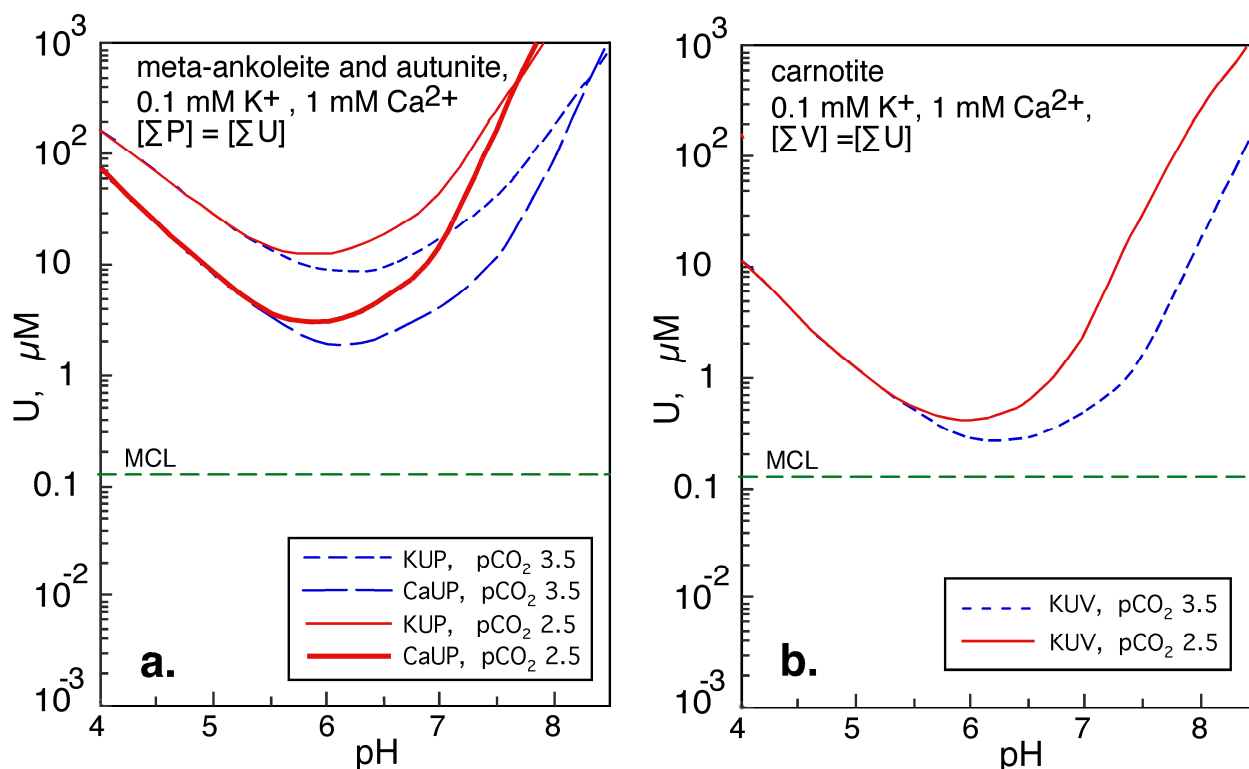


**Figure 3.** pH dependence of U and V concentrations when both elements are derived solely from mineral dissolution, with  $\text{K}^+ = 0.1 \text{ mM}$ ,  $\text{Ca}^{2+} = 1 \text{ mM}$ , and  $I = 100 \text{ mM}$ . (a.) Meta-ankoleite (KUP) and autunite (CaUP). (b.) Carnotite (KUV).

Under conditions of equal U and V concentrations, it is also important to consider the influence of  $\text{K}^+$ . Being a component of carnotite, like V, elevated  $\text{K}^+$  concentrations will suppress U concentrations. The influence of varying  $\text{K}^+$  on U concentrations is presented in Figure 4 for the cases of  $\text{pH} = 6.0$  and  $7.0$ ,  $\text{Ca}^{2+} = 1 \text{ mM}$ , at  $p\text{CO}_2 = 3.5$  and  $2.5$ . These graphs illustrate predictions that the influence of carbonate and  $\text{Ca}^{2+}$  are minor at  $\text{pH} 6.0$ , and major at  $\text{pH} 7.0$ . The equilibrium calculations indicate that, with sub-mM levels of  $\text{K}^+$ , carnotite can control U slightly below its MCL at a moderate  $p\text{CO}_2$  of  $2.5$ , but that significantly higher  $\text{K}^+$  would be required at  $\text{pH} 7.0$  and elevated  $\text{CO}_2$ . Under these more adverse conditions, whether or not kinetic limitations will be

important in keeping U released from carnotite below the MCL in groundwaters remains to be determined.

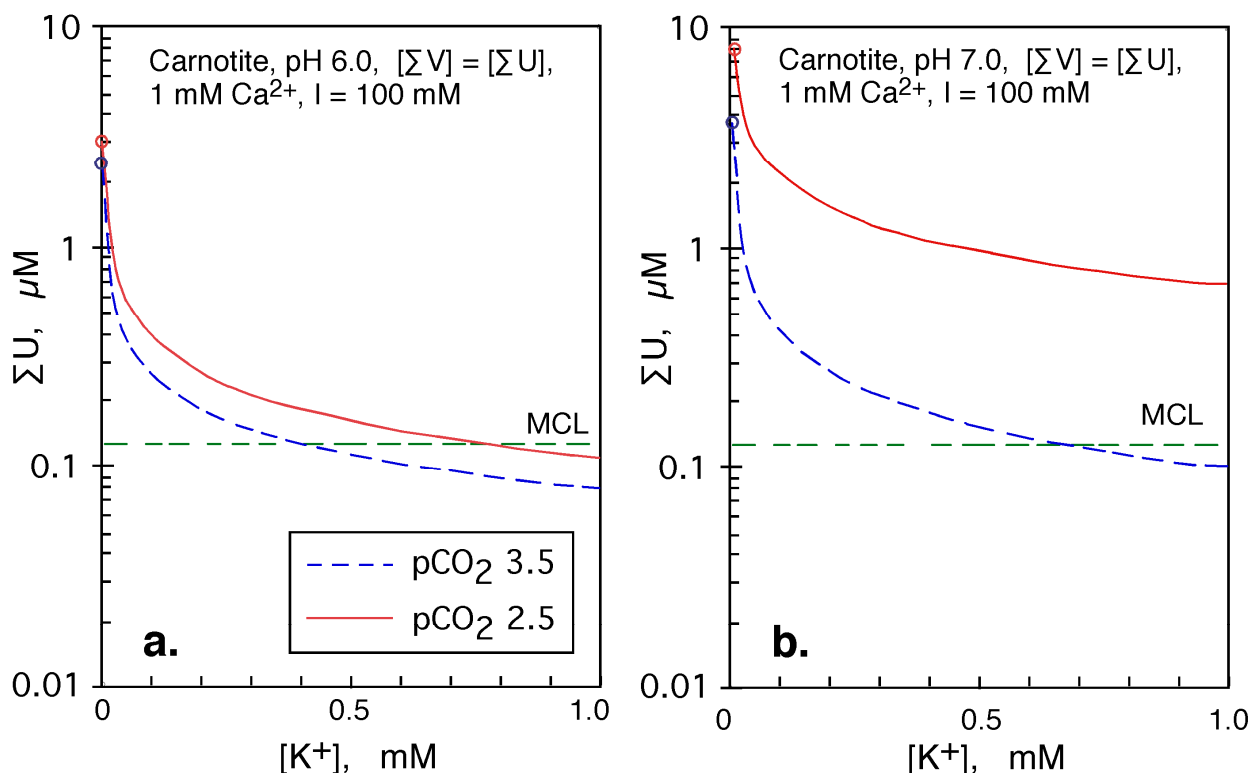


**Figure 4.** Dependence of U concentrations on  $K^+$  concentrations, for equilibrium with carnotite, with 1 mM  $Ca^{2+}$ ,  $[\Sigma V] = [\Sigma U]$ , for  $pCO_2 = 3.5$  and  $2.5$ , at (a.) pH 6.0, and (b.) pH 7.0. Open circles near the y-axes denote the upper limits for U and V, associated with the lower limits for K, at  $[K^+] = [\Sigma V] = [\Sigma U]$ .

**Batch experiments.** Measurements of homogeneous precipitation of U(VI) in aqueous solutions exhibited complex dependence on  $K^+$  and V(V) concentrations. Time trends for the influence of  $K^+$  concentrations on U(VI) precipitation at pH 6.0 and  $pCO_2 \approx 3.5$  are shown for V concentrations of 5 and 50  $\mu M$  in Figures 5a,b. For the pH 6.0 experiments, U concentrations decreased from concentrations initially ranging from 0.78 to 0.89  $\mu M$  to below the MCL (0.13  $\mu M$ ) in most cases tested. However, as shown later, measured U concentrations remained above equilibrium predictions over the

experimental timeframe of 50 days. It should be noted that the 10 mM  $K^+$  test with 5  $\mu M$  V(V) lowered the U concentration below the detection level (0.2 nM) by day 21. At the lower levels of 0.1 and 1.0 mM  $K^+$  tested, rates and extents of U removal were very similar. The reason for decreased U removal at higher concentrations of V was not identified. The small amount of U loss in control samples (0 mM  $K^+$ ) may have resulted from sorption onto walls of the vials.

Time trends for the influence of  $K^+$  concentrations on U(VI) precipitation at pH 7.8 and  $pCO_2 \approx 3.5$  are shown for V concentrations of 5 and 50  $\mu M$  in Figures 6a,b. It should be noted that the initial U concentration of 0.78  $\mu M$  is slightly lower than the predicted equilibrium levels of 0.83  $\mu M$  in the pH 7.8, 5  $\mu M$  V experiment (Figure 6a). However, even with higher  $K^+$  concentrations where calculations predict substantial carnotite precipitation, U concentrations remained elevated. Within the pH 7.8, 50  $\mu M$  V(V) series, U removal was effective, but the dependence on  $K^+$  concentration was again indistinct at and above 0.1 mM  $K^+$ .

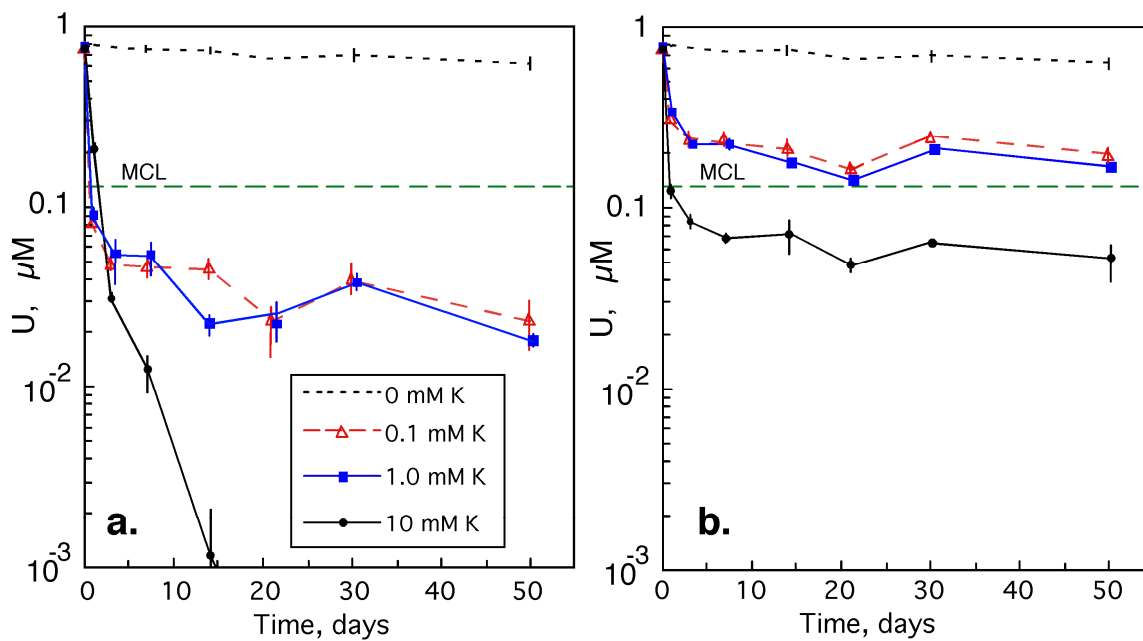


**Figure 5.** Time trends in U concentrations measured in pH 6.0,  $p\text{CO}_2 \approx 3.5$  solutions with  $\text{K}^+$  varied from 0 to 10 mM, and V(V) concentrations of (a.) 5  $\mu\text{M}$  and (b.) 50  $\mu\text{M}$ . Data points and vertical bars indicate averages and ranges of duplicates, respectively.

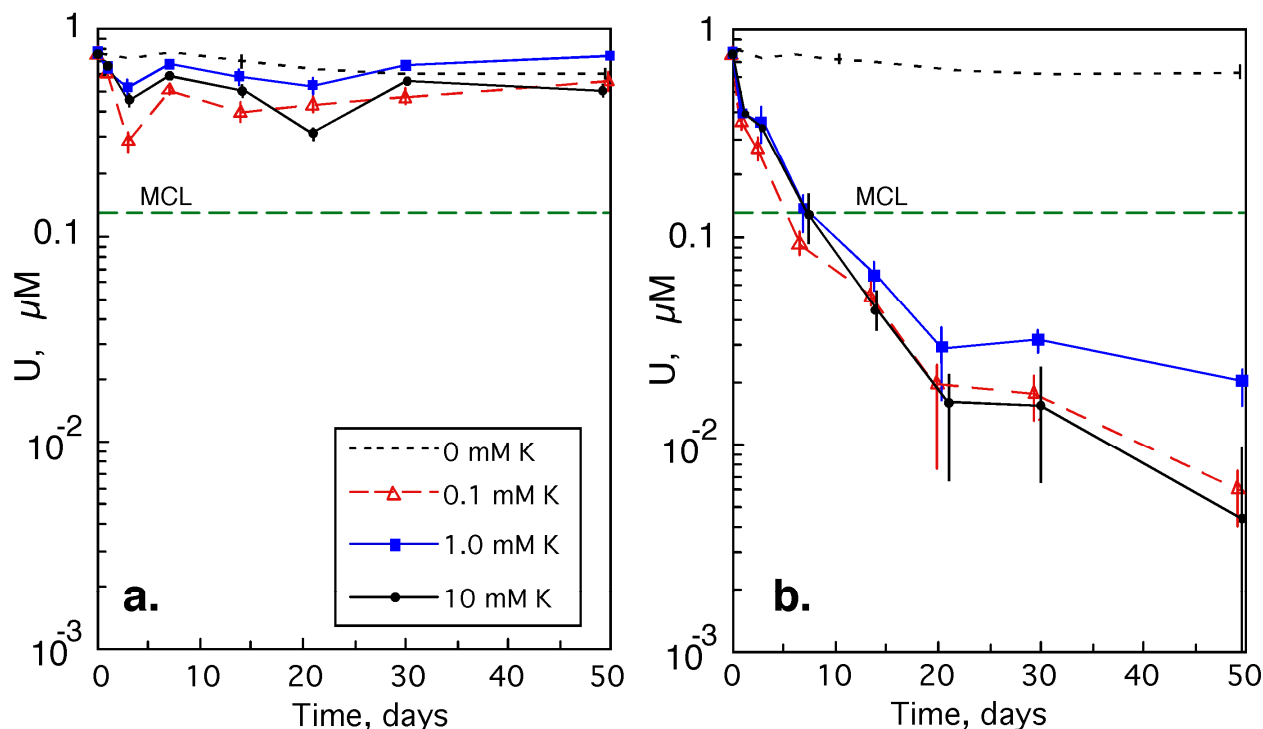


**Figure 6.** Time trends in U concentrations measured in pH 7.8,  $p\text{CO}_2 \approx 3.5$  solutions with  $\text{K}^+$  varied from 0 to 10 mM, and V(V) concentrations of (a.) 5  $\mu\text{M}$  and (b.) 50  $\mu\text{M}$ . Data points and vertical bars indicate averages and ranges of duplicates, respectively.

Because U removal at pH 6 with V(V) = 5  $\mu\text{M}$  was rapid and relatively similar for  $\text{K}^+$  = 0.1 and 1.0 mM, another set of pH 6 experiments was conducted with further variation of V around this lower concentration. These experiments yielded rapid U removal similar to results shown in Figure 5a. The lowest final U concentrations were obtained using initial V concentrations ranging from 2 to 10  $\mu\text{M}$ . Comparisons between all experimental results and thermodynamic predictions are summarized in Figure 7. The experiments conducted at pH 6.0 resulted in U concentrations below the MCL with V concentration up to 20  $\mu\text{M}$ . At higher V concentrations, the extent of U removal after



50 days was less effective in the tests conducted at pH 6. At pH 7.8, experiments with 5  $\mu\text{M}$  V showed little U variation with increased  $\text{K}^+$ , even with higher levels of  $\text{K}^+$  where predictions from carnotite solubilities are expected to drive U concentrations below the MCL. For the pH 7.8 experiments conducted with 50  $\mu\text{M}$  V, U concentrations dropped below the MCL with both 0.1 and 1.0 mM  $\text{K}^+$ .

The composition of the U-containing solid phase produced in these experiments was examined in a separate, 2 L batch solution. The precipitated solid was collected on 0.2  $\mu\text{m}$  filters and analyzed by inductively coupled plasma optical emission spectrometry (ICP-OES) and X-ray diffraction (XRD). The ICP-OES analysis of the acid-digested precipitate yielded a K:U:V ratio of 1.24:1.00:1.09, compared to an ideal ratio of 1:1:1 for carnotite. The solid phase was determined to be amorphous in the XRD measurement. Formation of an amorphous precipitate is consistent with Barton's earlier unsuccessful attempt at synthesizing carnotite crystals from aqueous phase solutions, which apparently prompted his choice of a high temperature method for fusing various uranyl salts with ammonium metavanadate (26). Despite the lack of crystallinity in our precipitate, the similar K:U:V elemental ratios and the approximate agreement of measured aqueous U concentrations with thermodynamic predictions support precipitation of a carnotite-like phase.

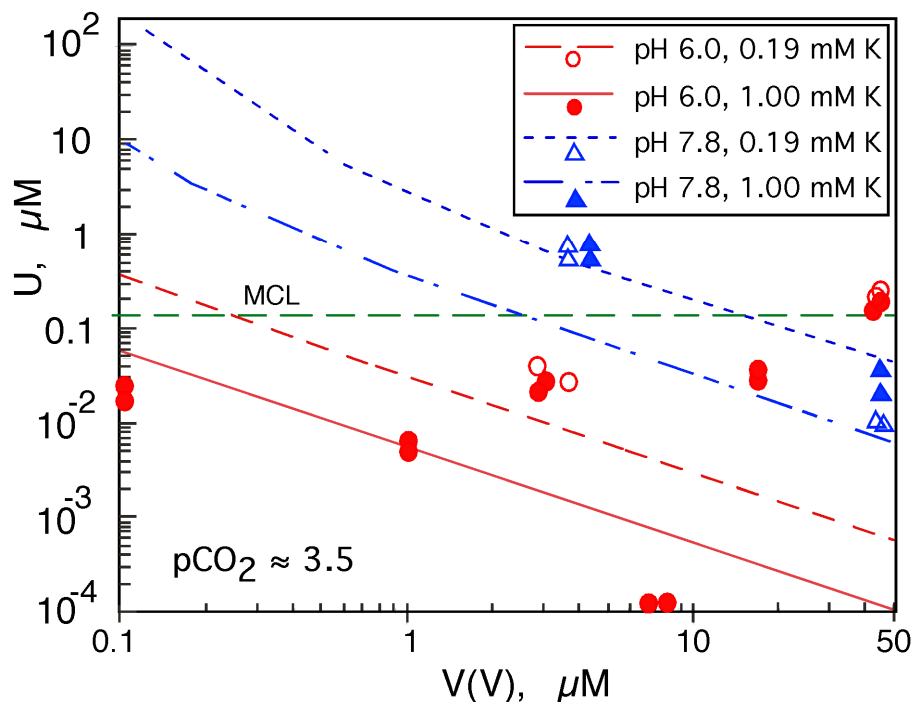


**Figure 7.** Comparisons of predicted (curves) and measured (data points at 50 days equilibration) dependence of U concentrations on V(V) concentrations at  $p\text{CO}_2 = 3.5$ , and  $\text{K}^+ = 0.19$  and  $1.0$  mM, for equilibrium with carnotite ( $\text{pH} = 6.0$  and  $7.8$ ).

**Implications and future studies.** These equilibrium calculations and experiments on U removal from aqueous solutions indicate that precipitation of a carnotite-like phase is a potentially viable strategy for treating some U-contaminated groundwaters. Because this approach does not rely on maintaining reduction of uraninite, the need for an indefinite supply of electron donor is circumvented. At  $\text{pH} \approx 6$ , additions of moderate levels of V(V) ( $< 2 \mu\text{M}$ ) and  $\text{K}^+$  ( $< 2$  mM) can precipitate with U(VI) in oxidizing solutions, leaving dissolved U concentrations below the MCL. The results from our batch experiments further demonstrate that the precipitation reaction could also be employed to extract (mine) U and V from groundwaters where they both occur at elevated

concentrations. From the work presented here, a combination of  $K^+$  addition and adjustment to  $pH \approx 6.0$  will precipitate carnotite-like solids, yielding about 10 kg U and 2 kg V per hectare-meter of groundwater when initial concentrations of these elements are 2  $\mu M$ . More U-contaminated solutions and sediments are being tested in batch and column experiments over a range of pH (5 to 7.5) and solution compositions (complexing agents and ionic strength) in our next stages of exploring the potential for K- and Ca-vanadate-based in-situ U remediation.

## Acknowledgments

Funding was provided through the Environmental Remediation Sciences Program of the Office of Biological and Environmental Research, U. S. Department of Energy, under contract No. DE-AC02-05CH11231. We thank the anonymous reviewers for their helpful comments.

## Literature Cited

1. Langmuir, D., *Aqueous Environmental Geochemistry*. Prentice-Hall: Upper Saddle River, NJ, 1997; p 600.
2. Lovley, D. R.; Phillips, E. J. P.; Gorby, Y. A.; Landa, E. R., Microbial reduction of uranium. *Nature* **1991**, *350*, 413-416.
3. Wall, J. D.; Krumholz, L. R., Uranium reduction. *Annual Review of Microbiology* **2006**, *60*, 149-166.
4. Wan, J.; Tokunaga, T. K.; Brodie, E. L.; Wang, Z.; Zheng, Z.; Herman, D. J.; Hazen, T. C.; Firestone, M. K.; Sutton, S. R., Reoxidation of bio-reduced uranium under reducing conditions. *Environ. Sci. Technol.* **2005**, *39*, (16), 6162-6169.
5. Luo, W.; Gu, B., Dissolution and mobilization of uranium in a reduced sediment by natural humic substances under anaerobic conditions. *Environ. Sci. Technol.* **2009**, *43*, (1), 152-156.
6. Tokunaga, T. K.; Wan, J.; Kim, Y.; Daly, R. A.; Brodie, E. L.; Hazen, T. C.; Herman, D.; Firestone, M. K., Influences of organic carbon supply rate on uranium bio-reduction in initially oxidizing, contaminated sediment. *Environ. Sci. Technol.* **2008**, *42*, (23), 8901-8907.

7. Wan, J.; Tokunaga, T. K.; Kim, Y.; Brodie, E.; Daly, R.; Hazen, T. C.; Firestone, M. K., Effects of organic carbon supply rates on mobility of previously bioreduced uranium in a contaminated sediment. *Environ. Sci. Technol.* **2008**, *42*, 7573-7579.
8. Casas, I.; Gimenez, J.; Marti, V.; Torrero, M. E.; de Pablo, J., Kinetic studies of unirradiated UO<sub>2</sub> dissolution under oxidizing conditions in batch and flow experiments. *Radiochimica Acta* **1994**, *66/67*, 23-27.
9. Finneran, K. T.; Housewright, M. E.; Lovley, D. R., Multiple influences of nitrate on uranium solubility during bioremediation of uranium-contaminated subsurface sediments. *Environ. Microbiol.* **2002**, *4*, 510-516.
10. Senko, J. M.; Istok, J. D.; Suflita, J. M.; Krumholz, L. R., In-situ evidence for uranium immobilization and remobilization. *Environ. Sci. Technol.* **2002**, *36*, 1491-1496.
11. Catalano, J. G.; McKinley, J. P.; Zachara, J. M.; Heald, S. M.; Smith, S. C.; Brown, G. E., Jr., Changes in uranium speciation through a depth sequence of contaminated Hanford sediments. *Environ. Sci. Technol.* **2006**, *40*, (8), 2517-2524.
12. Arey, J. S.; Seaman, J. C.; Bertsch, P. M., Immobilization of uranium in contaminated sediments by hydroxyapatite addition. *Environ. Sci. Technol.* **1999**, *33*, (2), 337-342.
13. Zheng, Z.; Wan, J.; Song, X.; Tokunaga, T. K., Sodium meta-autunite colloids: Synthesis, characterization, and stability. *Colloids and Surfaces A: Physicochemical and Engineering Aspects* **2006**, *274*, 48-55.
14. Wellman, D. M.; Catalano, J. G.; Icenhower, J. P.; Gerner, A. P., Synthesis and characterization of sodium meta-autunite, Na(UO<sub>2</sub>PO<sub>4</sub>)•3H<sub>2</sub>O. *Radiochimica Acta* **2005**, *93*, 393-399.
15. Martinez, R. J.; Beazley, M. J.; Taillefert, M.; Arakaki, A. K.; Skolnick, J.; Sobecky, P. A., Aerobic uranium (VI) bioprecipitation by metal-resistant bacteria isolated from radionuclide- and metal-contaminated subsurface soils. *Environ. Microbiol.* **2007**, *9*, (12), 3122-3133.
16. Jerden, J. L. J.; Sinha, A. K., Phosphate based immobilization of uranium in an oxidizing bedrock aquifer. *Appl. Geochem.* **2003**, *18*, 823-843.
17. Evans, H. T.; Garrels, R. M., Thermodynamic equilibria of vanadium in aqueous systems as applied to the interpretation of the Colorado Plateau ore deposits. *Geochimica Cosmochimica Acta* **1958**, *15*, 131-149.
18. Appleman, D. E.; Evans, H. T., The crystal structures of synthetic anhydrous carnotite, K<sub>2</sub>(UO<sub>2</sub>)<sub>2</sub>V<sub>2</sub>O<sub>8</sub>, and its cesium analogue, Cs<sub>2</sub>(UO<sub>2</sub>)<sub>2</sub>V<sub>2</sub>O<sub>8</sub>. *Am. Mineral.* **1965**, *50*, (7,8), 825-842.
19. Langmuir, D., Uranium solution-mineral equilibria at low temperatures with applications to sedimentary ore deposits. *Geochimica Cosmochimica Acta* **1978**, *42*, 547-569.
20. Wanty, R. B.; Goldhaber, M. B., Thermodynamics and kinetics of reactions involving vanadium in natural systems: Accumulation of vanadium in sedimentary rocks. *Geochimica Cosmochimica Acta* **1992**, *56*, 1471-1483.
21. Adriano, D. C., *Trace Elements in the Terrestrial Environment*. Springer-Verlag: New York, 1986; p 533.
22. Apodaca, L. E.; Mueller, D. K.; Kotterba, M. T. Review of trace element blank and replicate data collected in groundwater and surface water for the National Water-Quality Assessment Program, 1991-2002. [http://pubs.usgs.gov/sir/2006/5093/table\\_6.html](http://pubs.usgs.gov/sir/2006/5093/table_6.html)
23. E.P.A. *Contaminant Candidate List 3 Chemicals: Classification of the PCCL to CCL*,; 2008 February.

24. Peacock, C. L.; Sherman, D. M., Vanadium(V) adsorption onto goethite ( $\alpha$ -FeOOH) at pH 1.5 to 12: A surface complexation model based on ab initio molecular geometries and EXAFS spectroscopy. *Geochimica Cosmochimica Acta* **2004**, 68, (8), 1723-1733.
25. Dzombak, D. A.; Morel, F. M. M., *Surface Complex Modeling- Hydrous Ferric Oxide*. Wiley: New York, 1990; p 393.
26. Barton, P. B., Synthesis and properties of carnotite and its alkali analogues. *Am. Mineral.* **1958**, 43, (9,10), 799-817.
27. Finch, R.; Murakami, T., Systematics and paragenesis of uranium minerals. In *Uranium: Mineralogy, Geochemistry, and the Environment.*, Burns, P. C.; Finch, R., Eds. Mineralogical Society of America: Washington, DC, 1999; Vol. 38, pp 91-179.
28. Parkhurst, D. L.; Appelo, C. A. J., User's Guide to PHREEQC (Version 2)--A Computer Program for Speciation, Batch-Reaction, One-Dimensional Transport, and Inverse Geochemical Calculations. [http://wwwbrr.cr.usgs.gov/projects/GWC\\_coupled/phreeqc/](http://wwwbrr.cr.usgs.gov/projects/GWC_coupled/phreeqc/) **2005**.
29. Guillaumont, R.; Fanghanel, T.; Fuger, J.; Grenthe, I.; Neck, V.; Palmer, D. A.; Rand, M. H.; Mompean, F. J.; Illemassene, M.; Domenechi-Orti, C., *Update on the Chemical Thermodynamics of Uranium, Neptunium, Plutonium, Americium, and Technetium*. Elsevier: Amsterdam, 2003; Vol. 5.
30. Dong, W.; Brooks, S. C., Determination of the formation constants of ternary complexes of uranyl and carbonate with alkaline earth metals ( $\text{Mg}^{2+}$ ,  $\text{Ca}^{2+}$ ,  $\text{Sr}^{2+}$ , and  $\text{Ba}^{2+}$ ) using anion exchange method. *Environ. Sci. Technol.* **2006**, 40, (15), 4689-4695.
31. Larson, J. W., Thermochemistry of vanadium(5+) in aqueous solutions. *J. Chem. Eng. Data* **1995**, 40, (6), 1276-1280.
32. Rai, D.; Xia, Y.; Rao, L.; Hess, N. J.; Felmy, A. R.; Moore, D. A.; McCready, D. E., Solubility of  $(\text{UO}_2)_3(\text{PO}_4)_2 \cdot 4\text{H}_2\text{O}$  in  $\text{H}^+$  - $\text{Na}^+$  - $\text{OH}^-$  - $\text{H}_2\text{PO}_4^-$  - $\text{HPO}_4^{2-}$  - $\text{PO}_4^{3-}$  - $\text{H}_2\text{O}$  and its comparison to the analogous  $\text{PuO}_2^{2+}$  system. *J. Solution Chem.* **2005**, 34, (4), 469-498.
33. Good, N. E.; Winget, G. D.; Winter, W.; Connolly, T. N.; Izawa, S.; Singh, R. M. M., Hydrogen ion buffers for biological research. *Biochemistry* **1966**, 5, (2), 467-477.
34. Giammar, D. E.; Hering, J. G., Equilibrium and kinetic aspects of soddyite dissolution and secondary phase precipitation in aqueous suspension. *Geochimica Cosmochimica Acta* **2004**, 68, (18), 3235-3245.